

Chiral extrapolation of nucleon axial charge g_A in effective field theory^{*}

Hong-na Li (李洪娜)^{1,2;1)} P. Wang (王平)^{1,3;2)}

¹ Institute of High Energy Physics, Chinese Academy of Sciences, Beijing 100049, China

² College of Physics, Jilin University, Changchun, Jilin 130012, China

³ Theoretical Physics Center for Science Facilities, Chinese Academy of Sciences, Beijing 100049, China

Abstract: The extrapolation of nucleon axial charge g_A is investigated within the framework of heavy baryon chiral effective field theory. The intermediate octet and decuplet baryons are included in the one loop calculation. Finite range regularization is applied to improve the convergence in the quark-mass expansion. The lattice data from three different groups are used for the extrapolation. At physical pion mass, the extrapolated g_A are all smaller than the experimental value.

Keywords: chiral extrapolation, nucleon axial charge, effective field theory, finite range regularization

PACS: 12.39.Fe, 14.20.Dh, 12.38.Gc **DOI:** 10.1088/1674-1137/40/12/123106

1 Introduction

The nucleon axial charge, g_A , is a fundamental property of the nucleon, which reveals how the up and down quark intrinsic spins contribute to the spin of the proton and neutron, governing β decay and providing a quantitative measure of spontaneous chiral symmetry breaking in low energy hadronic physics. The axial charge g_A is of great importance to any further calculation of hadron structure.

The axial charge g_A is defined as the axial vector form factor at zero four-momentum transfer, $g_A = G_A(0)$. The axial vector form factor is given by the nucleon matrix element of the axial vector current, $A_\mu^a = \bar{\psi}\gamma_\mu\gamma_5(\tau^a/2)\psi$, with u, d quark doublet ψ , $\langle N(p', s') | A_\mu^3 | N(p, s) \rangle = i\bar{u}(p', s')[\gamma_\mu\gamma_5 G_A(q^2) + \frac{q_\mu}{2M_N}\gamma_5 G_P(q^2)]\frac{\tau^3}{2}u(p, s)$, where G_P is the induced pseudoscalar form factor, τ^a is an isospin Pauli matrix, and $q_\mu = p'_\mu - p_\mu$ is the momentum transfer. At zero momentum transfer, the axial charge g_A is the spin difference between u and d quarks in the proton, i.e.

$$g_A = \Delta u - \Delta d. \quad (1)$$

Experimentally, g_A has been obtained very precisely through neutron β decay, with the Particle Data Group value $g_A = 1.27 \pm 0.003$ [1]. Theoretically, there are many calculations in different methods, such as the cloudy bag model [2], the perturbative chiral quark model [3],

the relativistic constituent quark model [4], Schwinger-Dyson formalism [5], chiral perturbation theory [6], etc. There are also many lattice simulations of axial charge [7–12]. Due to the limitations of computing ability, all the simulations of g_A are at large quark mass. The obtained g_A at large quark mass are smaller than the experimental data. Therefore, it is interesting to see how the axial charge g_A changes at low pion mass.

In this paper, we will extrapolate nucleon axial charge g_A in the framework of heavy baryon chiral perturbation theory with finite range regularization (FRR). FRR has been applied in the extrapolation of nucleon mass, magnetic form factors, strange form factors, charge radii, first moments, etc [13–27]. It is proved that FRR can provide good convergent behaviour of pion mass expansion. Therefore, it is expected to have a good description of the pion mass dependence of axial charge g_A over a wide range of pion mass.

2 Nucleon axial charge

The lowest-order chiral Lagrangian including the octet and decuplet baryons is expressed as

$$L_v = i\text{Tr}\bar{B}_v(v\cdot\mathcal{D})B_v + 2D\text{Tr}\bar{B}_v S_v^\mu \{A_\mu, B_v\} + 2F\text{Tr}\bar{B}_v S_v^\mu [A_\mu, B_v] - i\bar{T}_v^\mu(v\cdot\mathcal{D})T_{v\mu} + C(\bar{T}_v^\mu A_\mu B_v + \bar{B}_v A_\mu T_v^\mu), \quad (2)$$

Received 17 August 2016

^{*} Supported by National Natural Science Foundation of China (11475186) and Sino-German CRC 110 (NSFC 11621131001)

1) E-mail: lihongna@ihep.ac.cn

2) E-mail: pwang4@ihep.ac.cn



Content from this work may be used under the terms of the Creative Commons Attribution 3.0 licence. Any further distribution of this work must maintain attribution to the author(s) and the title of the work, journal citation and DOI. Article funded by SCOAP³ and published under licence by Chinese Physical Society and the Institute of High Energy Physics of the Chinese Academy of Sciences and the Institute of Modern Physics of the Chinese Academy of Sciences and IOP Publishing Ltd

where S_v^μ is the covariant spin operator defined as

$$S_v^\mu = \frac{i}{2} \gamma^5 \sigma^{\mu\nu} v_\nu. \quad (3)$$

Here, v^ν is the nucleon four-velocity. In the rest frame, we have $v^\nu = (1, 0, 0, 0)$. D , F and C are the standard $SU(3)$ -flavour coupling constants.

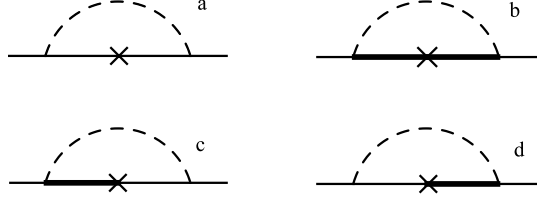


Fig. 1. The one-loop Feynman diagrams for calculating the quark contribution to the proton spin. The thin and thick solid lines are for the octet and decuplet baryons, respectively.

According to the Lagrangian, the one-loop Feynman diagrams, which contribute to axial charge g_A of the proton, are plotted in Fig. 1. The axial charge is the spin difference between u and d quark. The contributions of the u- and d-quark sector to the proton spin, from Fig. 1a, are expressed as

$$\Delta u^a = [C_{N\pi} I_{2\pi}^{NN} + C_{\Sigma K} I_{2K}^{N\Sigma} + C_{\Lambda\Sigma K} I_{5K}^{N\Lambda\Sigma} + C_{N\eta} I_{2\eta}^{NN}] s_u, \quad (4)$$

$$\Delta d^a = \left[\frac{7}{2} C_{N\pi} I_{2\pi}^{NN} + \frac{1}{5} C_{\Sigma K} I_{2K}^{N\Sigma} - C_{\Lambda\Sigma K} I_{5K}^{N\Lambda\Sigma} - \frac{1}{4} C_{N\eta} I_{2\eta}^{NN} \right] s_d, \quad (5)$$

where the coefficients, C are expressed as

$$C_{N\pi} = -\frac{(D+F)^2}{288\pi^3 f_\pi^2}, \quad (6)$$

$$C_{\Sigma K} = -\frac{5(D-F)^2}{288\pi^3 f_\pi^2}, \quad (7)$$

$$C_{\Lambda\Sigma K} = \frac{(D-F)(D+3F)}{288\pi^3 f_\pi^2}, \quad (8)$$

$$C_{N\eta} = -\frac{2}{3} \frac{(3F-D)^2}{288\pi^3 f_\pi^2}. \quad (9)$$

The tree level contributions to the proton spin from u and d quark of intermediate octet baryons are used in the above formulas. For example, for the intermediate proton and neutron, their spins are expressed as

$$s_p = \frac{4}{3} s_u - \frac{1}{3} s_d, \quad s_n = \frac{4}{3} s_d - \frac{1}{3} s_u. \quad (10)$$

s_u and s_d are the single quark spin of u and d quark. With the $SU(2)$ symmetry, $s_u = s_d = s_q$ and s_q can be written as

$$s_q(m_\pi^2) = c_0 + c_2 m_\pi^2 + c_4 m_\pi^4, \quad (11)$$

where c_0 , c_2 and c_4 are the low energy constants.

The contribution of u-, d-quark sector to the proton spin, described by diagram (b) of Fig. 1, are expressed as

$$\Delta u^b = [C_{\Delta\pi} I_{2\pi}^{N\Delta} + C_{\Sigma^* K} I_{2K}^{N\Sigma^*}] s_u, \quad (12)$$

$$\Delta d^b = \left[\frac{2}{7} C_{\Delta\pi} I_{2\pi}^{N\Delta} + \frac{1}{5} C_{\Sigma^* K} I_{2K}^{N\Sigma^*} \right] s_d. \quad (13)$$

where the coefficients $C_{\Delta\pi}$ and $C_{\Sigma^* K}$ are

$$C_{\Delta\pi} = \frac{35C^2}{648\pi^3 f_\pi^2}, \quad (14)$$

$$C_{\Sigma^* K} = \frac{5}{28} C_{\Delta\pi}. \quad (15)$$

Similar to the case of the octet intermediate state, the tree level quark contributions to the spin of decuplet baryons are also used. For example

$$s_{\Delta^+} = 2s_u + s_d, \quad s_{\Sigma^{*-}} = 2s_d + s_s. \quad (16)$$

Diagrams (c) and (d) of Fig. 1 provide contributions from intermediate states involving an octet-decuplet transition. The u-, d-quark-sector contribution to the proton spin from these diagrams are expressed as

$$\Delta u^{c+d} = [C_{N\Delta\pi} I_{3\pi}^{N\Delta} + C_{\Sigma\Sigma^* K} I_{5K}^{N\Sigma\Sigma^*} + C_{\Lambda\Sigma^* K} I_{5K}^{N\Lambda\Sigma^*}] \times s_u, \quad (17)$$

$$\Delta d^{c+d} = \left[-C_{N\Delta\pi} I_{3\pi}^{N\Delta} + \frac{1}{5} C_{\Sigma\Sigma^* K} I_{5K}^{N\Sigma\Sigma^*} - C_{\Lambda\Sigma^* K} I_{5K}^{N\Lambda\Sigma^*} \right] s_d. \quad (18)$$

where

$$C_{N\Delta\pi} = -\frac{(D+F)C}{27\pi^3 f_\pi^2}, \quad (19)$$

$$C_{\Sigma\Sigma^* K} = -\frac{5}{8} \frac{(D-F)C}{27\pi^3 f_\pi^2}, \quad (20)$$

$$C_{\Lambda\Sigma^* K} = -\frac{1}{8} \frac{(D+3F)C}{27\pi^3 f_\pi^2}. \quad (21)$$

The integrals in the above equations, $I_{2j}^{\alpha\beta}$, $I_{5j}^{\alpha\beta\gamma}$ and $I_{3j}^{\alpha\beta}$ are defined in Ref. [15].

The total u-, d- quark sector contributions to the spin of the proton are written as

$$\Delta u = Z \left[\frac{4}{3} (c_0 + c_2 m_\pi^2 + c_4 m_\pi^4) + \Delta u^a + \Delta u^b + \Delta u^{c+d} \right],$$

$$\Delta d = Z \left[-\frac{1}{3} (c_0 + c_2 m_\pi^2 + c_4 m_\pi^4) + \Delta d^a + \Delta d^b + \Delta d^{c+d} \right], \quad (22)$$

where Z is the wave function renormalization constant, expressed as

$$Z = 1 / \left[1 + \frac{1}{48\pi^3 f_\pi^2} (\beta_\pi^{NN} I_{2\pi}^{NN} + \beta_\pi^{N\Delta} I_{2\pi}^{N\Delta} + \beta_K^{N\Lambda} I_{2K}^{N\Lambda} + \beta_K^{N\Sigma} I_{2K}^{N\Sigma} + \beta_K^{N\Sigma^*} I_{2K}^{N\Sigma^*} + \beta_\eta^{NN} I_{2\eta}^{NN}) \right]. \quad (23)$$

The above coefficients are expressed as

$$\begin{aligned} \beta_\pi^{NN} &= \frac{9}{4}(D+F)^2, & \beta_\pi^{N\Delta} &= 2C^2 \\ \beta_K^{N\Lambda} &= \frac{1}{4}(3F+D)^2, & \beta_K^{N\Sigma} &= \frac{9}{4}(D-F)^2 \\ \beta_K^{N\Sigma^*} &= \frac{1}{2}C^2, & \beta_\eta^{NN} &= \frac{1}{4}(3F-D)^2. \end{aligned} \quad (24)$$

The K- and η - meson masses have relationships with the pion mass as

$$m_K^2 = \frac{1}{2}m_\pi^2 + m_K^2|_{\text{phy}} - \frac{1}{2}m_\pi^2|_{\text{phy}}, \quad (25)$$

$$m_\eta^2 = \frac{1}{3}m_\pi^2 + m_\eta^2|_{\text{phy}} - \frac{1}{3}m_\pi^2|_{\text{phy}}. \quad (26)$$

This enable a direct relationship between the nucleon axial charge and the pion mass. By fitting the lattice data with different pion mass, we can get the low energy constants c_0 , c_2 and c_4 .

In our calculation, the one-gluon-exchange is also included. Although it lies outside the framework of chiral effective field theory, the effect of one-gluon-exchange (OGE) is particularly important for spin dependent quantities. Hogaason and Myhrer [28] showed that the incorporation of the exchange current correction arising from the effective one-gluon-exchange (OGE) force shifts the tree-level non-singlet charge, g_A , from $\frac{5}{3}s_q$ to $\frac{5}{3}s_q - G$, where G is about 0.05. The OGE correction shifts the tree-level singlet charge g_0 from s_q to $s_q - 3G$. In other words, the spin of each constituent quark gain a OGE correction $-G$ at tree level.

3 Numerical results

In the numerical calculations, the couplings constant D and F are $D = 0.8$, $F = 0.46$. The decuplet coupling C is chosen to be -1.2 as in Ref. [29]. The regulator in the integrals is chosen to be of a dipole form

$$u(k) = \frac{1}{(1+k^2/\Lambda^2)^2}, \quad (27)$$

with $\Lambda = 0.8$ GeV. This regulator has been used in our previous study of nucleon mass, magnetic form factors, strange form factors, charge radii, first moments, etc [13–27].

In Fig. 2, the pion mass dependence of g_A with $\Lambda = 0.8$ GeV is shown for lattice data of Ref. [7]. The dotted, dashed and solid lines are for tree level, loop and total contribution, respectively. At large pion mass, the axial charge g_A changes little. At small pion mass, g_A decreases with the decreasing pion mass. Compared with the pion mass dependence of proton magnetic form factors [15, 23], at low pion mass, the curvature is small and opposite. This is because the leading diagram in the case of magnetic form factor has no contribution for g_A . At physical pion mass, the extrapolated g_A is 1.10, which is smaller than the experimental value 1.27.

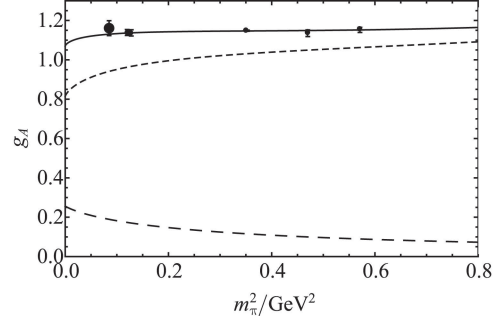


Fig. 2. g_A fitted by the lattice data of Ref. [7] at $\Lambda = 0.8$. The dotted, dashed and solid lines are for the tree level, loop and total contribution, respectively.

To provide an estimate of the uncertainty in these results, we vary the regulator parameter, Λ , governing the size of meson cloud contributions to proton structure. Considering $\Lambda = 0.8 \pm 0.2$ GeV, the obtained low energy constants c_0 , c_2 , c_4 as well as the quark spin at physical pion mass are listed in Table 1. By varying Λ , we can provide an error bar for g_A . For example, the highest and lowest g_A at physical pion mass are 1.14 ($0.805 - (-0.333)$) and 1.07 ($0.772 - (-0.302)$). From the table, one can see that the loop/tree contribution increases/decreases with the increasing Λ . The highest and lowest value of g_A versus pion mass as well as the central value of g_A are shown in Fig. 3. It is clear that the extrapolated g_A with error bar is still smaller than the experimental value.

There are also other lattice groups simulating the axial charge g_A . Figure 4 and Fig. 5 are results for the lattice data from Refs. [8–9]. The same as in Fig. 3, the lines in the middle are for $\Lambda = 0.8$ GeV. The upper and lower lines are obtained by varying Λ from 0.6 to 1 GeV. The extrapolated g_A from Ref. [8] at physical pion mass is $1.12_{-0.03}^{+0.03}$. The lattice data from Ref. [9] varied a lot with the change of the pion mass though the extrapolated g_A at physical pion mass is a little larger than the other two lattice groups. At large pion mass, Fig. 4 and Fig. 5 show that g_A changes quickly with the increasing pion mass for the data of ETMC and data from Ref. [9]. This is because, different from the data of LHPC, there is no con-

straint from these lattice data at large pion mass. Overall, one can see the results from different lattice groups are comparable and all the extrapolated g_A at physical pion mass are smaller than the experimental values,

within the error bars. The obtained results with central $\Lambda = 0.8$ GeV for these three lattice groups are listed in Table 2.

Table 1. The parameters fitted by the lattice data of Ref. [7] and the obtained quark spin of the proton at physical pion mass for the regulator parameter $\Lambda = 0.6, 0.8, 1.0$ GeV.

Λ/GeV	c_0	c_2/GeV^{-2}	c_4/GeV^{-4}	Z	Δu	Δd	g_A	tree	loops
0.6	0.74	-0.04	0.04	0.84	0.80	-0.30	1.107	0.99	0.12
0.8	0.77	-0.09	0.07	0.71	0.79	-0.32	1.104	0.87	0.23
1.0	0.81	-0.12	0.09	0.58	0.77	-0.33	1.106	0.75	0.36

Table 2. The parameters fitted by three group lattice data [7–9] and the obtained quark spin of the proton at physical pion mass for the regulator parameter $\Lambda = 0.8$ GeV.

lattice data	c_0	c_2/GeV^{-2}	c_4/GeV^{-4}	Z	Δu	Δd	tree	loops	g_A with error bar
Ref. [7]	0.77	-0.09	0.07	0.71	0.79	-0.32	0.87	0.23	$1.10^{+0.04}_{-0.03}$
Ref. [8]	0.78	-0.21	0.60	0.71	0.80	-0.32	0.88	0.24	$1.12^{+0.03}_{-0.03}$
Ref. [9]	0.83	-0.06	-0.20	0.71	0.85	-0.34	0.94	0.25	$1.19^{+0.04}_{-0.03}$

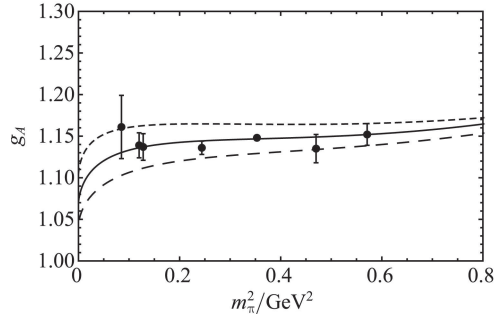


Fig. 3. Error band of g_A fitted by the lattice data of Ref. [7]. The upper (dotted) line is for the upper limit with $g_A = \Delta u(\Lambda = 0.6 \text{ GeV}) - \Delta d(\Lambda = 1.0 \text{ GeV})$. The middle (solid) line is for the central value of g_A ($\Lambda = 0.8 \text{ GeV}$). The lower (dashed) line is for the lower limit with $g_A = \Delta u(\Lambda = 1.0 \text{ GeV}) - \Delta d(\Lambda = 0.6 \text{ GeV})$.

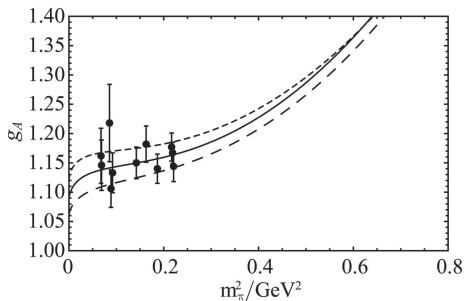


Fig. 4. Error band of g_A fitted by the lattice data of Ref. [8]. The upper (dotted) line is for the upper limit with $g_A = \Delta u(\Lambda = 0.6 \text{ GeV}) - \Delta d(\Lambda = 1.0 \text{ GeV})$. The middle (solid) line is for the central value of g_A ($\Lambda = 0.8 \text{ GeV}$). The lower (dashed) line is for the lower limit with $g_A = \Delta u(\Lambda = 1.0 \text{ GeV}) - \Delta d(\Lambda = 0.6 \text{ GeV})$.

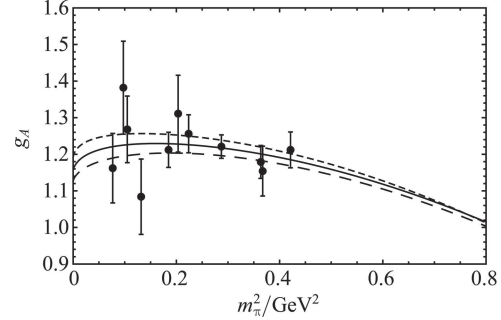


Fig. 5. Error band of g_A fitted by the lattice data of Ref. [9]. The upper (dotted) line is for the upper limit with $g_A = \Delta u(\Lambda = 0.6 \text{ GeV}) - \Delta d(\Lambda = 1.0 \text{ GeV})$. The middle (solid) line is for the central value of g_A ($\Lambda = 0.8 \text{ GeV}$). The lower (dashed) line is for the lower limit with $g_A = \Delta u(\Lambda = 1.0 \text{ GeV}) - \Delta d(\Lambda = 0.6 \text{ GeV})$.

4 Summary

In summary, we extrapolated the axial charge g_A in chiral effective field theory with finite range regularisation. The dipole regulator is used as our previous extrapolation for nucleon mass, form factors, first moments, etc. The lattice data are from three lattice groups where the volume corrections are given explicitly. Different from the proton magnetic form factor, the axial charge g_A decreases with decreasing pion mass when m_π is small. The lattice data over a wide pion mass range can be well described with the FRR chiral effective field theory. At physical pion mass, the extrapolated g_A are comparable to each other and all of them are smaller than the

experimental value. To estimate the error bars for the extrapolation, we vary Λ in the regulator from 0.6 to 1 GeV. The upper limit of the extrapolated g_A at physical pion mass is still smaller than the experimental value.

We should mention that the volume correction is given by the lattice groups. It will be interesting to extrapolate the lattice data directly without volume correction in finite volume chiral effective field theory.

References

- 1 J. Beringer et al (Particle Data Group Collaboration), Phys. Rev. D, **86**: 010001 (2012)
- 2 S. D. Bass and A. W. Thomas, Phys. Lett. B, **684**: 216 (2010)
- 3 X. Y. Liu, K. Khosonthongkee, A. Limphirat et al, Phys. Rev. D, **91**: 034022 (2015)
- 4 S. Boffi, L. Y. Glozman, W. Klink et al, Eur. Phys. J. A, **14**: 17 (2002)
- 5 N. Yamanaka, S. Imai, T. M. Doi et al, Phys. Rev. D, **89**: 074017 (2014)
- 6 V. Bernard, Prog. Part. Nucl. Phys., **60**: 82 (2008)
- 7 J. D. Bratt et al (LHPC Collaboration), Phys. Rev. D, **82**: 094502 (2010)
- 8 C. Alexandrou et al (ETM Collaboration), Phys. Rev. D, **83**: 045010 (2011)
- 9 S. Capitani, M. Della Morte, G. von Hippel et al, Phys. Rev. D, **86**: 074502 (2012)
- 10 R. G. Edwards et al (LHPC Collaboration), Phys. Rev. Lett., **96**: 052001 (2006)
- 11 S. Ohta (RBC and UKQCD Collaborations), PoS LATTICE, **2013**: 274 (2014)
- 12 T. Yamazaki et al (RBC+UKQCD Collaboration), Phys. Rev. Lett., **100**: 171602 (2008)
- 13 R. D. Young, D. B. Leinweber, and A. W. Thomas, Prog. Part. Nucl. Phys., **50**: 399 (2003)
- 14 D. B. Leinweber, A. W. Thomas, and R. D. Young, Phys. Rev. Lett., **92**: 242002 (2004)
- 15 P. Wang, D. B. Leinweber, A. W. Thomas et al, Phys. Rev. D, **75**: 073012 (2007)
- 16 P. Wang and A. W. Thomas, Phys. Rev. D, **81**: 114015 (2010)
- 17 C. R. Allton, W. Armour, D. B. Leinweber et al, Phys. Lett. B, **628**: 125 (2005)
- 18 W. Armour, C. R. Allton, D. B. Leinweber et al, Nucl. Phys. A, **840**: 97 (2010)
- 19 J. M. M. Hall, D. B. Leinweber, and R. D. Young, Phys. Rev. D, **88**: 014504 (2013)
- 20 D. B. Leinweber et al, Phys. Rev. Lett., **94**: 212001 (2005)
- 21 P. Wang, D. B. Leinweber, A. W. Thomas et al, Phys. Rev. C, **79**: 065202 (2009)
- 22 P. Wang, D. B. Leinweber, A. W. Thomas et al, Phys. Rev. D, **79**: 094001 (2009)
- 23 P. Wang, D. B. Leinweber, A. W. Thomas et al, Phys. Rev. D, **86**: 094038 (2012)
- 24 P. Wang, D. B. Leinweber, and A. W. Thomas, Phys. Rev. D, **89**: 033008 (2014)
- 25 J. M. M. Hall, D. B. Leinweber and R. D. Young, Phys. Rev. D, **89**: 054511 (2014)
- 26 P. Wang, D. B. Leinweber, and A. W. Thomas, Phys. Rev. D, **92**: 034508 (2015)
- 27 H. Li, P. Wang, D. B. Leinweber et al, Phys. Rev. C, **93**: 045203 (2016)
- 28 H. Hogaasen and F. Myhrer, Phys. Rev. D, **37**: 1950 (1988)
- 29 E. E. Jenkins, M. E. Luke, A. V. Manohar et al, Phys. Lett. B, **302**: 482 (1993); **388**: 866 (1996)